Sodium as densification aid in $MgAl_2O_4$ nanoceramics

Isabella L. M. Costa[§], Joice Miagava[†,§], Ricardo H. R. Castro[§,*]

[§]*Department of Materials Science and Engineering, University of California–Davis, One Shields Avenue, Davis, CA 95616, United States*

[†]*Insper Institute of Education and Research, Sao Paulo-SP, 04546-042, Brazil*

*Corresponding Author: rhrcastro@ucdavis.edu

Abstract

Magnesium aluminate nanoceramics show superior hardness due to an extension of the Hall-Petch relationship down to grain sizes below 10 nm. However, the manufacturing of nanoceramics with such exceedingly small grains constitutes a significant challenge. This work proposes sodium as an effective dopant to reduce the processing requirements to achieve full densification with inhibited coarsening. Using Spark Plasma Sintering, we produced fully dense transparent Na-doped $MgAl_2O_4$ under 400 MPa at 1000°C with grain sizes below 15 nm. Na-doped samples achieved toughness (K_{IC}) as high as 5.23 MPa/m$^{1/2}$, surpassing values characteristic of undoped $MgAl_2O_4$ with a similar grain size, 3.57 MPa/m$^{1/2}$. The role of Na^+ as a sintering aid is briefly discussed.

Keywords: $MgAl_2O_4$, magnesium aluminate, hardness, SPS, sintering

Introduction

Recent works show the hardness of nanocrystalline Magnesium Aluminate Spinel ($MgAl_2O_4$, MAS) may surpass single-crystal sapphire with similar transparency, making it a promising candidate for transparent armors [1,2]. Optimal performance results when the microstructure is fully dense since residual pores may compromise mechanical properties and reduce transparency by acting as light scattering centers. Sintering ceramics to fully dense bodies while maintaining grains at the nanoscale constitutes a significant processing challenge. The application of high pressures to increase the pore elimination while shortening the overall sintering time is among the effective strategies to obtain dense nanoceramics. However, maintaining grain sizes below 20 nm still requires very high pressures, typically beyond 850 MPa [1–3], representing a significant engineering challenge for scaling up.

In this work, we investigate the role of sodium (Na^+) as a new sintering additive to fabricate nanocrystalline MAS using High-Pressure Spark Plasma Sintering (HPSPS). Like Li^+, an effective sintering aid for MAS [4], Na^+ reduced the pressure needed for densification with significant coarsening inhibition to 400 MPa. MAS with grain sizes below 15 nm showed hardness comparable to undoped MAS and transparency above 60% in the infrared spectrum. The novel doped nanoceramics also showed improved toughness, likely due to the segregation of Na^+ to interfaces.

Experimental procedures

MAS nanoparticles were synthesized using the coprecipitation method, with Na^+ being incorporated using NaOH, as detailed in the Supplemental Information. The obtained powders were degassed in a vacuum (0.08 mmHg) for 16 h at 400 °C and kept in a glove box before sintering. The SiC/Diamond (Versimax®) HPSPS die was assembled inside the glovebox and quickly transferred to a Dr. Sinter model 825S, Syntex, Japan. **Table S1** in Supplemental Information shows the heating and loading cycles used during the HPSPS tests.

The surface area of the powders was quantified using a Gemini VII Micromeritics Instrument Corp., Norcross, GA, USA. X-ray Diffraction (Bruker-AXS D8 Advance) with Cu Kα radiation informed crystallographic structure and crystallite sizes using whole profile fitting (Rietveld refinement). Transmission Electron Microscopy (JEOL JEM 2100F-AC) was used for microstructural characterization and Electron Microprobe Analysis (Cameca SX-100) for chemical composition. Archimedes method (ASTM B311-13) was applied to determine the density of the sintered bodies.

Hardness was measured using a Vickers diamond pyramid indenter (Mitutoyo HM-220A, following the ASTM C1327-15) under 60 *gf* at 0.015 mm/s. Loading time, holding, and unloading were 4 s, 15 s, 4 s, respectively. 10-15 indentations without spallation were imaged under SEM (Thermo Fisher FEI. Nova NanoSEM430) and used to quantify dimensions for the Vickers hardness and toughness calculations. Thermo Scientific Evolution 220 Spectrometer was used to investigate the UV-Vis-IR transmittance spectrum.

Results and discussion

Figure 1a shows the XRD patterns for MAS powders doped with Na^+ contents ranging from 0 to 10.9 at%. Broad peaks are consistent with nanoscale dimensions, and the single-phase is identified as the expected spinel structure (group Fd-3m). **Figure 1b** shows a reduction in surface area but no particular crystallite size growth trend as a function of Na^+ content - crystallites remained at 5.6 ±0.3 nm. The behavior indicates that the surface area reduction results from particle aggregation rather than grain enlargement.

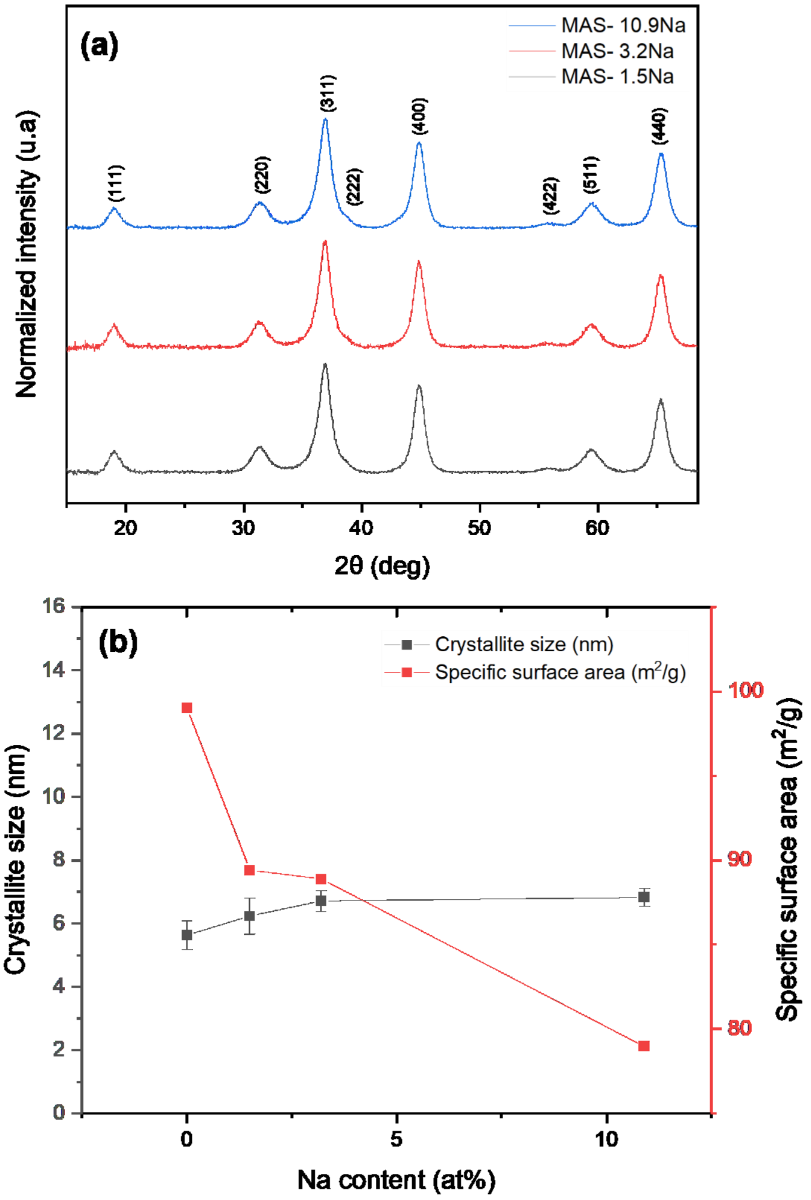

Figure 1. (a) XRD patterns for as-synthesized MAS powders doped with Na^+. (b) Crystallite sizes and BET specific surface area as a function of Na^+ content.

Following the protocols listed in **Table S1**, the powders were sintered under HPSPS. The diffraction patterns in **Figure 2a** indicate the spinel structure is dominant in all pellets. We observe a narrowing of the peaks compared to the powder patterns, indicating coarsening. Low-intensity peaks at 42.89° and 62.19° are characteristic of MgO (group Fm-3m) and show in all doped pellets. Traces of MgO suggest Na^+ may be substituting Mg^{2+} in the structure, leading to segregation of Mg^{2+} to grain boundaries and subsequent nucleation of MgO. That behavior would be similar to Li^+ doped MAS, which substitutes Mg^{2+} at concentrations above 1.8 mol%.[5] A substitution would generate oxygen vacancies following an equation equivalent to that proposed by Talimian et al.[5] for Li^+ in MAS:

$$Na_2O \xrightarrow{2MgAl_2O_4} 2Na_{Mg}^{|} + 4V_{Al}^{|||} + O_O^X + 7V_O^{oo} \qquad (1)$$

Since oxygen is the rate-limiting species in MAS diffusion, the formation of vacancies increases the diffusion, improving densification.[6,7]

Figures 2b and **2c** show crystallite sizes and densities as a function of sintering pressure for all pellets sintered at 1000 and 1100 °C. The higher temperature led to increased grain size and densification. A decrease in grain size and increase in densification follow the Na^+ increase for the same sintering conditions. While the densification trend is consistent with the discussed diffusion model, the grain growth inhibition may be reflecting drag forces caused by the traces of MgO. The conditions to obtain fully dense undoped MAS with grain sizes of ~13 nm were 920 °C and 1.4 GPa, consistently with the literature. [1] The same microstructure was obtained at a significantly lower pressure when doping with 10.9 at% Na, at 1000 °C, and 400 MPa.

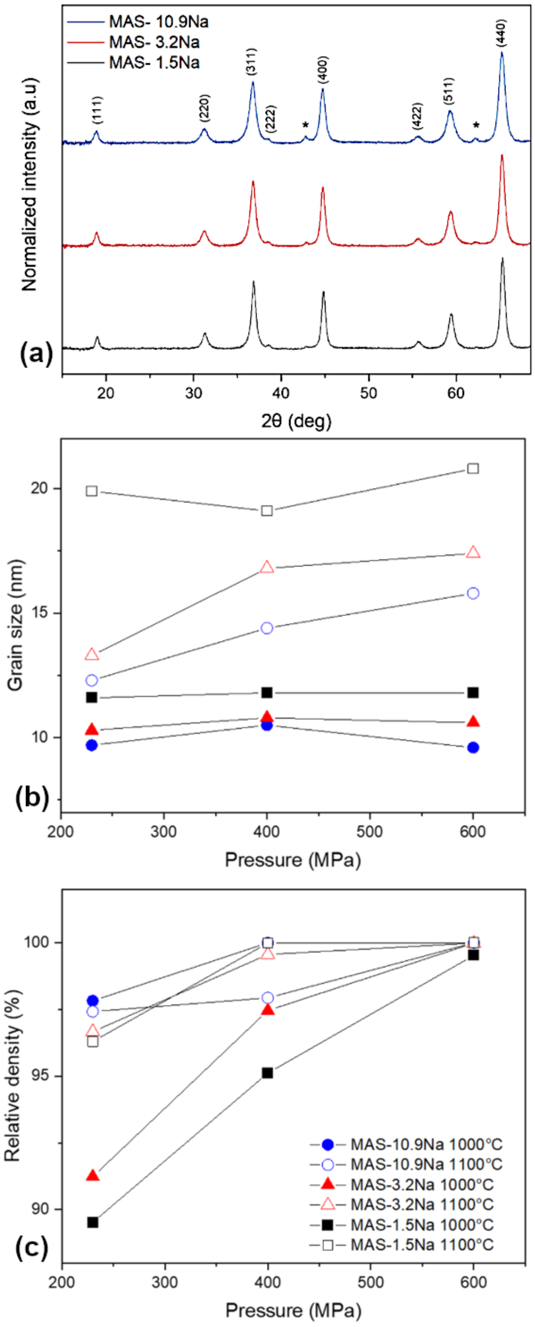

Figure 2. (a) Representative examples of X-ray diffraction patterns for sintered Na-doped MAS. The patters refer to samples sintered at 1000 °C and 600 MPa. The stars indicate the characteristic MgO peaks (space group Fm-3m). (b) Crystallite size as a function of sintering pressure; (c) relative density as a function of sintering pressure.

Pressure and temperature significantly impacted the optical properties and directly reflected the density trends, as seen in **Figure 3a**. Since pores act as light scattering centers, samples with residual porosity were generally more opaque. **Figure 3b** shows TEM images for 10.9 at% Na sintered at 1000 °C. The microstructures reveal crystalline structures, with well-defined grain boundaries, and grains in a size range consistent with the crystallite sizes in **Figure 2b**. Sizes are uniform, and there is no evidence of porosity. The transmission spectrum of this pellet is shown in **Figure 3c** and indicates limited transmittance.[17] The transmission increases for larger wavelengths, reaching up to 63% in the infrared region.

While MAS shows intrinsically high transparency [8,9], the traces of MgO may be responsible for light scattering. Part of the light absorption may also be related to the yellow shade found in the pellets. Although coloration in SPS pellets has been attributed to residual graphite [10], HPSPS has been reported to produce color-free transparent MAS successfully. [1] Alternatively, Pathak et al. showed that oxygen vacancies cause a yellow color shift in MAS. [9] This explanation aligns with the high volume of vacancies expected with Na^+ doping.

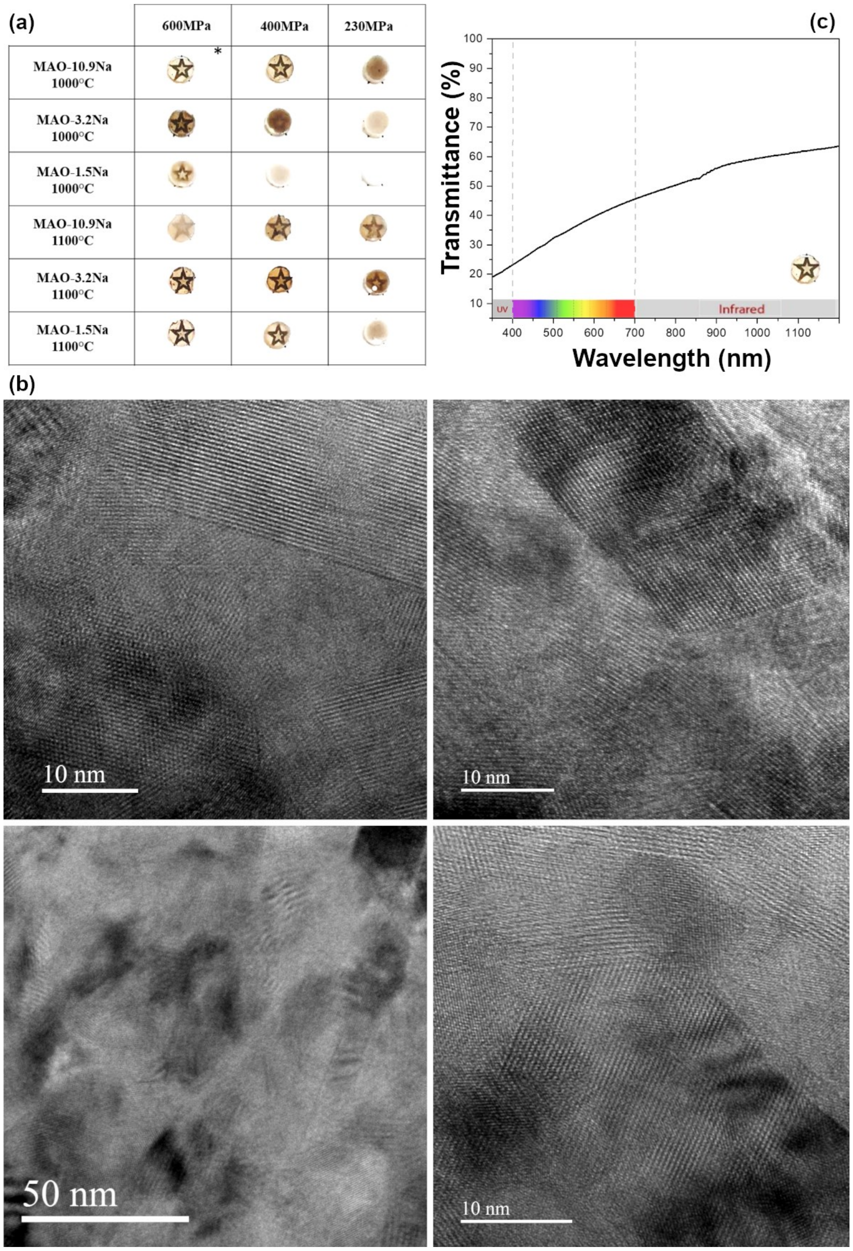

Figure 3. (a) Na-MAS pellets photographs - the star is printed on the paper underneath. (b) TEM images and (c) transmission spectrum for a 10.9 at% Na-MAS pellet sintered at 1000°C and 600MPa (pellet thickness is 0.78 mm).

Figure 4 shows Vickers hardness for the denser pellets produced in our study and data by Sokol et al.[2] and Muche et al.[1]. Undoped MAS achieved hardness of 24.2 GPa, consistent with

Muche et al., and demonstrating an extension of the Hall-Petch relation. The contrast with Sokol et al.[2] is due to stoichiometric differences.[11] Our samples' Mg:Al ratio is 1: 1.87, revealing an excess of Mg. Chiang and Kingery [12] reported that non-stoichiometry in $MgAl_2O_4$ accumulates around grain boundaries, affecting their intrinsic properties. We speculate the Mg excess is causing the strengthening of grain boundaries and postponing grain sliding/shearing, which would drive the inverse Hall-Petch behavior [13].

Doping of MAS with 1.5 at% Na-MAS resulted in pellets with similar hardness as the undoped. However, an increase in Na^+ content up to 10.9 at% resulted in slight softening. The behavior is consistent with a more pronounced second-phase fraction weakening the grain boundary regions through local defects.

The diagonal cracks of the indentations provided K_{1C} toughness values of 5.23±0.59 $MPa/m^{1/2}$ and 4.45±0.46$MPa/m^{1/2}$ for 1.5 and 10.9 at% Na-MAS, respectively. The results are higher than for undoped MAS with similar grain size, 3.57 $MPa/m^{1/2}$, and equivalent literature reports [14]. That shows Na^+ and associated defects impact crack propagation, consistent with recent reports connecting fracture energies to hardness in nanoceramics [15].

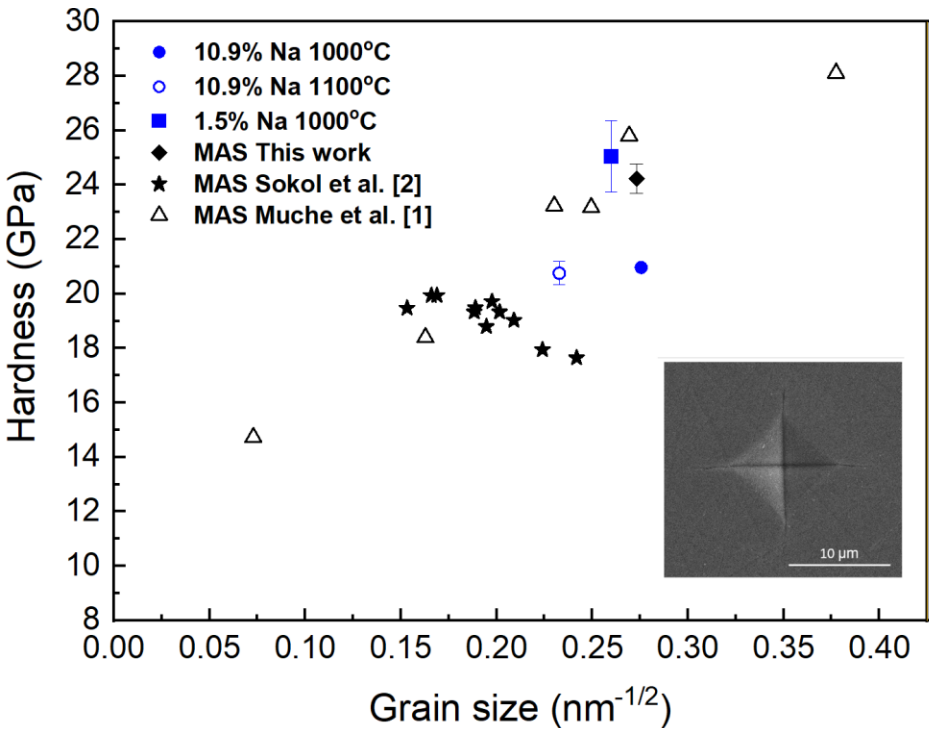

Figure 4. Vickers hardness for undoped and Na-MAS along with literature data. Inset shows a typical indentation imprint.

Conclusion

Na^+ is an effective additive for the sintering of nanocrystalline MAS, causing a reduction on the required pressure to achieve complete densification and grain sizes below 15 nm. The improved sintering was attributed to the formation of oxygen vacancies at the grain boundary regions. The doping caused the formation of MgO traces, which affected transparency. Vickers hardness and toughness reported for Na-MAS are equivalent or superior to undoped MAS.

Acknowledgments

This work was funded by the Army Research Office Grant W911NF1810361.

References

[1] D.N.F. Muche, J.W. Drazin, J. Mardinly, S. Dey, R.H.R. Castro, Colossal grain boundary strengthening in ultrafine nanocrystalline oxides, Mater. Lett. 186 (2017) 298–300. https://doi.org/10.1016/j.matlet.2016.10.035.

[2] M. Sokol, M. Halabi, Y. Mordekovitz, S. Kalabukhov, S. Hayun, N. Frage, An inverse Hall-Petch relation in nanocrystalline MgAl2O4 spinel consolidated by high pressure spark plasma sintering (HPSPS), Scr. Mater. 139 (2017) 159–161. https://doi.org/10.1016/j.scriptamat.2017.06.049.

[3] H. Ryou, J.W. Drazin, K.J. Wahl, S.B. Qadri, E.P. Gorzkowski, B.N. Feigelson, J.A. Wollmershauser, Below the Hall-Petch Limit in Nanocrystalline Ceramics, ACS Nano. 12 (2018) 3083–3094. https://doi.org/10.1021/acsnano.7b07380.

[4] I. Reimanis, H.-J. Kleebe, A Review on the Sintering and Microstructure Development of Transparent Spinel (MgAl2O4), J. Am. Ceram. Soc. 92 (2009) 1472–1480. https://doi.org/https://doi.org/10.1111/j.1551-2916.2009.03108.x.

[5] A. Talimian, H.F. El-Maghraby, M. Michálková, D. Galusek, Sintering and grain growth behaviour of magnesium aluminate spinel: Effect of lithium hydroxide addition, J. Eur. Ceram. Soc. 41 (2021) 5634–5643. https://doi.org/10.1016/j.jeurceramsoc.2021.05.003.

[6] K.P.R. REDDY, A.R. COOPER, Oxygen Diffusion in Magnesium Aluminate Spinel, J. Am. Ceram. Soc. 64 (1981) 368–371. https://doi.org/10.1111/j.1151-2916.1981.tb10304.x.

[7] Y. Oishi and Ken Ando, Self-diffusion of oxygen in polycrystalline MgAl2O4, J. Chem. Phys. 63 (2008) 376–378. https://doi.org/10.7868/s0044453717020303.

[8] C. Wang, Z. Zhao, Transparent MgAl2O4 ceramic produced by spark plasma sintering,

Scr. Mater. 61 (2009) 193–196. https://doi.org/https://doi.org/10.1016/j.scriptamat.2009.03.039.

[9] N. Pathak, P.S. Ghosh, S.K. Gupta, S. Mukherjee, R.M. Kadam, A. Arya, An Insight into the Various Defects-Induced Emission in MgAl2O4 and Their Tunability with Phase Behavior: Combined Experimental and Theoretical Approach, J. Phys. Chem. C. 120 (2016) 4016–4031. https://doi.org/10.1021/acs.jpcc.5b11822.

[10] J. Chen, S. Wang, M.S. Whittingham, Hydrothermal synthesis of cathode materials, J. Power Sources. 174 (2007) 442–448.

[11] L.E. Sotelo Martin, R.H.R. Castro, Al excess extends Hall-Petch relation in nanocrystalline zinc aluminate, J. Am. Ceram. Soc. 105 (2022) 1417–1427. https://doi.org/https://doi.org/10.1111/jace.18176.

[12] Y. -M Chiang, W.D. Kingery, Grain-Boundary Migration in Nonstoichiometric Solid Solutions of Magnesium Aluminate Spinel: II, Effects of Grain-Boundary Nonstoichiometry, J. Am. Ceram. Soc. 73 (1990) 1153–1158. https://doi.org/10.1111/j.1151-2916.1990.tb05172.x.

[13] A.G. Sheinerman, R.H.R. Castro, M.Y. Gutkin, A model for direct and inverse Hall-Petch relation for nanocrystalline ceramics, Mater. Lett. 260 (2020) 126886. https://doi.org/10.1016/j.matlet.2019.126886.

[14] J.A. Wollmershauser, B.N. Feigelson, E.P. Gorzkowski, C.T. Ellis, R. Goswami, S.B. Qadri, J.G. Tischler, F.J. Kub, R.K. Everett, An extended hardness limit in bulk nanoceramics, Acta Mater. 69 (2014) 9–16.

[15] A. Bokov, J.B. Rodrigues Neto, F. Lin, R.H.R. Castro, Size-induced grain boundary energy increase may cause softening of nanocrystalline yttria-stabilized zirconia, J. Am.

Ceram. Soc. 103 (2020) 2001–2011. https://doi.org/10.1111/jace.16886.